

# Heteroepitaxial Growth of ZnS on GaP

I. BERTÓTI, M. FARKAS-JAHNKE, E. LENDVAY, T. NÉMETH

*Research Institute for Technical Physics of the Hungarian Academy of Sciences, Budapest, Hungary*

*Received 4 February 1969*

Epitaxial layers of ZnS were grown on GaP single crystals by a chemical transport reaction. The growth process and the heterostructures obtained were investigated by X-ray diffraction and optical microscopy. It was found that the epitaxial overgrowth is polarity dependent. The formation of a transition layer at the interface between the ZnS and GaP was observed.

## 1. Introduction

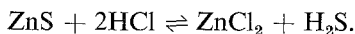
The heteroepitaxial growth of elementary semiconductors and  $A^{III}B^V$  compounds has been investigated by many authors, whereas considerably less papers on  $A^{II}B^{VI}$  compounds have been published and only a few of them deal with the epitaxial growth of ZnS [1-4].

The ZnS has two modifications: the hexagonal (wurtzite) which is stable above  $1050^\circ\text{C}$  and the cubic (sphalerite) which is stable below this temperature. Considering epitaxial growth, GaP seemed to be a very suitable substrate for ZnS, since its crystal structure is also cubic, its lattice parameter ( $a_{\text{GaP}} = 5.450 \text{ \AA}$ ) does not differ considerably from that of the ZnS ( $a_{\text{ZnS}} = 5.406 \text{ \AA}$ ), both compounds are of similar bond type, and they are able to form mixed crystals in all proportions [5].

## 2. Experimental

### 2.1. The Chemical Transport of ZnS

For the epitaxial growth of ZnS the well-known closed-tube chemical transport method using HCl as transport material was applied. The main chemical equilibrium reaction is:



This reaction is endothermic. Taking into consideration the dissociation equilibrium  $\text{H}_2\text{S} \rightleftharpoons \text{H}_2 + 0.5 \text{S}_2$ , in the range of the growth temperature the calculated equilibrium constants are:

$$\begin{aligned} \log K_{1000^\circ\text{K}} &= -1.9 \\ \log K_{1200^\circ\text{K}} &= -0.25 \end{aligned}$$

### 2.2. Procedure of the Layer Growth

The epitaxial growth was carried out in an evacuated and sealed quartz tube of 20 mm diameter and of  $30 \text{ cm}^3$  volume, placed in a horizontal two-zone furnace.

The source material was ZnS powder which had been previously fired, or crystals of luminescence purity. As substrates GaP crystals grown from Ga melt were used. Details of the preparation and morphology of these GaP crystals are described elsewhere [6]. The surface of the substrates was chemically treated in  $\text{HCl-H}_2\text{O}_2$  solution prior to ZnS deposition. During growth the substrates were held at a temperature between  $740$  and  $880^\circ\text{C}$ , while the temperature of the ZnS source surpassed this by about  $50^\circ\text{C}$ . The concentration of transport material was  $0.7 \text{ mg HCl/cm}^3$  added in the form of  $\text{NH}_4\text{Cl}$ . The mean rate of the epitaxial growth of ZnS amounted to  $5$  to  $20 \mu\text{m/h}$ . The method described also proved suitable for growing GaP layers on ZnS.

### 3. Initial Stage of the Epitaxial Growth

X-ray diffraction investigations showed that plate-like GaP substrates grown from Ga melt have extended polar  $\{111\}$  planes as well as facets with  $\{111\}$  and  $\{100\}$  orientation [6].

On the most extended  $\{111\}$  GaP surfaces the epitaxial growth of ZnS begins in the form of triangular prisms or hexagonal pyramids. All the triangular ZnS islands are of the same orientation, the direction of their bases being  $\langle 110 \rangle$ , while the apex of each triangle is  $\langle 211 \rangle$ . The tangential growth rates are different on the two types of

polar  $\{111\}$  surfaces. On  $(\bar{1}\bar{1}\bar{1})$  P-surfaces the growth starts by forming triangular islands quickly covering the whole surface. On the  $(111)$  Ga-surfaces, however, the tangential growth rate of the islands might be compared with the growth rate normal to the plane. Consequently, separated triangular prisms have been developed. After a longer growth process, however, continuous layers might form on the  $(111)$  surfaces, too. According to the X-ray investigations this latter overgrowth was occasionally microcrystalline, whereas only single crystal diffraction patterns were obtained from the layers grown on the  $(\bar{1}\bar{1}\bar{1})$  surfaces. Along the edges and tips of the substrate a faster growth was observed.

Microscopic investigations showed that in the initial stage of the process the substrate also reacts with the transport material before its complete coverage has been achieved.

Coincident etch structures appeared, mechanically separating the ZnS and GaP layers along the heterojunction, on both sides of the separated interfaces.

#### 4. Orientation of the Layers

To investigate the orientation and lattice structure of the overgrown layers simultaneously, X-ray rotational patterns were taken using  $\text{CuK}\alpha$  radiation. In each case the rotation axis was chosen perpendicular to the substrate plane in question. According to the X-ray patterns, the lattice was not always cubic but rather hexagonal or 6H polytype in spite of the low temperature of growth. Reflections on fig. 1 are characteristic of the hexagonal structure of the layer. On the patterns obtained, besides the sharp reflections, diffuse lines connecting some of the reflections were also visible. It is known that for ZnS crystals these lines are caused by stacking faults of the lattice, which are oriented perpendicular to the hexagonal  $c$ -axis, i.e. to one of the four possible cubic  $\langle 111 \rangle$  axes. The  $\langle 111 \rangle$  directions, distinguished by the stacking faults, were determined for all layers. It was found that the planes of stacking faults were always parallel to one of the Ga-covered planes, i.e. to the  $(111)$  basal, or the  $\{\bar{1}\bar{1}1\}$  lateral planes of the substrate. Therefore, the plane of the stacking faults in the layers grown on  $\{111\}$  planes covered with P atoms was parallel to one of the Ga-covered neighbouring planes.

The distinguished  $\langle 111 \rangle$  axes (or  $c$ -axes) in the layers grown on the  $\{100\}$  lateral planes, form

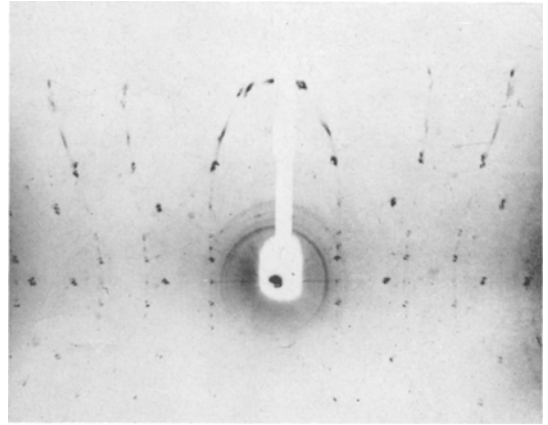


Figure 1 X-ray diffraction pattern of the epitaxially grown ZnS layer on  $(\bar{1}\bar{1}\bar{1})$  GaP plane. The reflections of both the ZnS and the GaP are visible on the pattern.

an angle of  $54^\circ 40'$  to the normal of this substrate plane, as was determined by the pattern displayed in fig. 2, measuring the angle between the diffuse line and the equator of the pattern. A simple epitaxial relationship can also be established by characterising the stacking faulted structure by cubic indices: the overgrown layer has the same Miller indices as the exposed GaP surface.

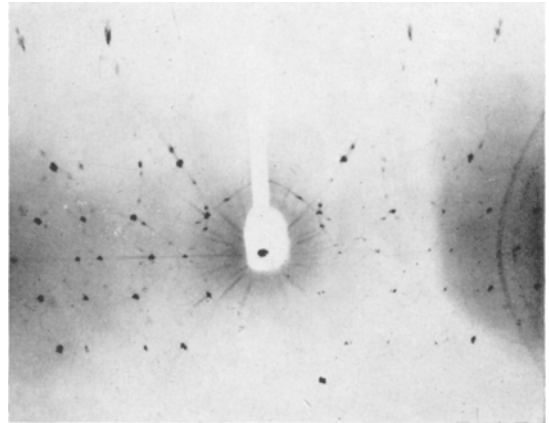


Figure 2 X-ray diffraction pattern of the epitaxially grown ZnS layer on  $\{100\}$  GaP surface.

#### 5. Defect Structure of the Layers

Microscopic examination of the ZnS layers showed some types of imperfections besides the stacking faults detected by X-rays.



Figure 3 Microcracks in ZnS layers epitaxially grown on  $(\bar{1}\bar{1}\bar{1})$  GaP surface (approx.  $\times 15$ ).

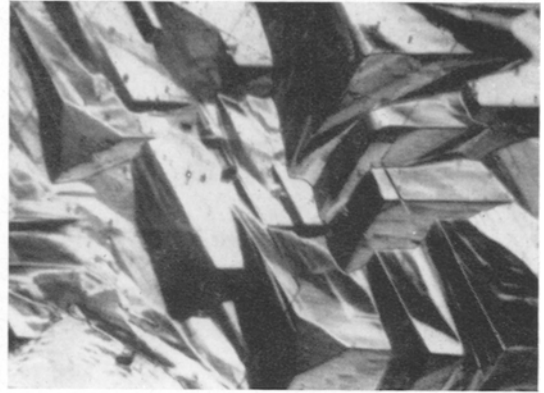


Figure 5 Characteristic growth pattern of ZnS on  $(\bar{1}\bar{1}\bar{1})$  GaP surfaces (approx.  $\times 48$ ).

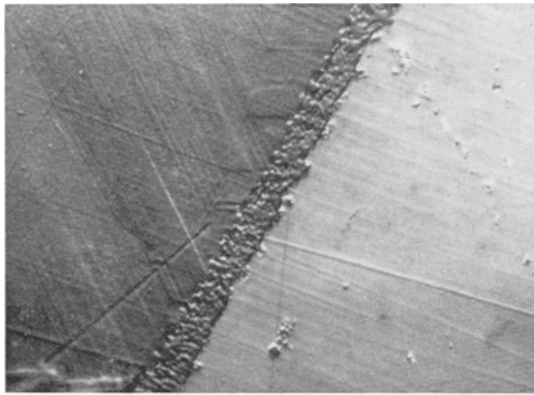


Figure 4 Angle-lapped section of GaP-ZnS interface after selective chemical etching. Between the ZnS (dark area) and GaP a transition layer is visible. On the ZnS side slip traces are developed (approx.  $\times 216$ ).

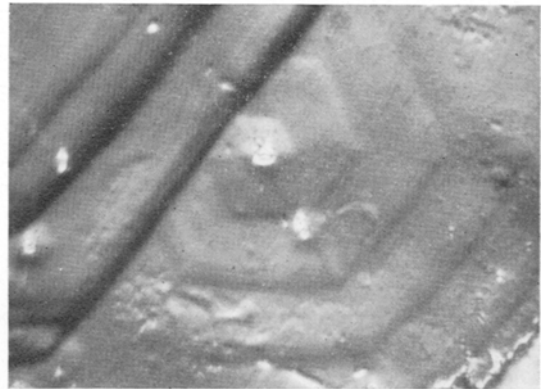


Figure 6 Growth spiral on the S-layer of the epitaxially grown ZnS (approx.  $\times 432$ ).

### 5.1. Deformation Effects

Generally the ZnS layers showed oriented microcracks, independently of whether they formed continuous layers or islands. A characteristic example is shown in fig. 3. The planes of the microcracks in the layers are perpendicular to the extended  $\{111\}$  planes, and coincide with the well-known  $\{110\}$  cleavage planes of ZnS and GaP as was proved by the X-ray investigations. Examining angle-lapped sections after chemical etching in chromic acid, slip traces forming  $60^\circ$  angles with each other were observable on the ZnS side of the heterostructure (fig. 4).

### 5.2. Defects in the Layers

Many growth features could be observed on as-grown  $\{111\}$  surfaces even before etching. Generally, on P-surfaces a characteristic tri-

angular pattern was formed as shown in fig. 5. Many polygonised growth spirals in conjunction with the screw dislocations were also observed on the layer surfaces. A typical spiral can be seen in fig. 6. For selective chemical etching of ZnS layers, aqueous chromic acid proved to be suitable [7, 8]. After etching, further screw dislocations were observed in the  $\langle 111 \rangle$  directions, the density of which was estimated from the etch patterns to be  $5 \times 10^3$  to  $5 \times 10^4/\text{cm}^2$ . The etch pits of the epitaxially grown ZnS on  $(\bar{1}\bar{1}\bar{1})$  GaP are generally of conical shape, ordered in certain directions. As seen in fig. 7 these are probably  $\langle 110 \rangle$  directions.

### 6. Transition Layer

Examining the heterostructure cross-section by microscopical methods a transition layer between the ZnS and GaP was observed in most cases.

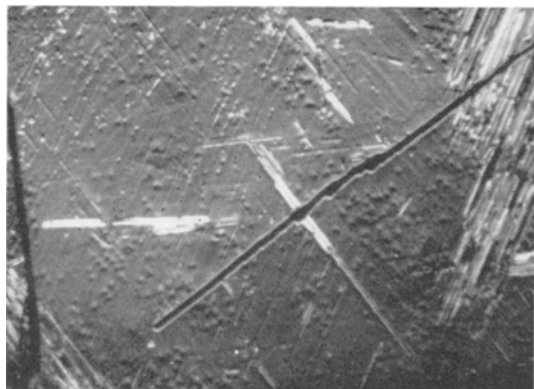


Figure 7 Etch pits oriented along the slip directions on the epitaxial ZnS layer grown on  $(\bar{1}\bar{1}\bar{1})$  GaP (approx.  $\times 456$ ).

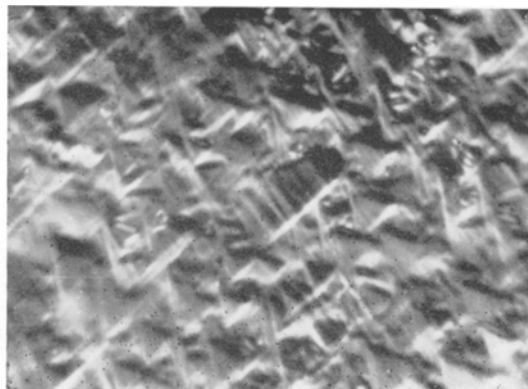


Figure 8 Etch pattern of the transition region between the GaP and ZnS (approx.  $\times 432$ ).

After selective etching the cross-sections perpendicular to the heterojunction plane exhibited a deep valley of 1 to 2  $\mu\text{m}$  width at the junction. For detailed investigations an angle-lapped section of  $5^\circ$  was made for enlarging this transition region to 10 to 15  $\mu\text{m}$  (see fig. 4). If this surface has high indices and the emerging transition region tends towards a direction with low indices, for instance the direction of one of the natural edges, the transition layer has a sharp boundary, both on the GaP and ZnS sides. Inside the transition region a triangular etch pattern developed which could be observed neither on the ZnS nor on the GaP side. An enlarged part of the transition region from fig. 4 is shown in fig. 8, where the triangular pattern is visible.

## 7. Discussion

According to previous investigations the spreading layers on  $\{111\}$  surfaces have steps along the  $\{100\}$  and  $\{110\}$  planes [9]. Of the six  $\langle 211 \rangle$  growth directions lying in a  $(111)$  surface, three correspond to the fast growing  $\{100\}$  steps and the opposite three to the slow-growing  $\{110\}$  steps. Generally, the fast-growing steps are eliminated and the resulting growth pattern shows the triangular forms as observed in the present case.

Polarity dependence of growth was observed in cases of  $A^{\text{III}}B^{\text{V}}$  compounds as a consequence of the electronic state of the polar  $\{111\}$  surfaces, the growth conditions are more favourable on the B surfaces than on the A ones, as was stated previously [10]. This is probably the reason why the more perfect ZnS layer was grown on the B

surfaces of GaP. The conical etch pits developed on this perfect ZnS layer surface also proved the polarity of the overgrowth, e.g. the outer surface of the ZnS layer was covered by sulphur atoms, in accordance with previous results [7, 8, 11-13].

Comparing the temperature-dependence of the linear thermal expansion coefficients of ZnS and GaP, it was established that at the growth temperature, the lattice constants of the two compounds were nearly the same. This fact is very favourable from the point of view of the heteroepitaxy. Having cooled down the grown heterostructure to room temperature, the summarised difference between the lattice constants of the two layers can amount to 15  $\mu\text{m}$  for each cm, since the linear thermal expansion coefficients of ZnS and GaP are different ( $\alpha_{\text{ZnS}} = 6.5 \times 10^{-6}/^\circ\text{C}$ ;  $\alpha_{\text{GaP}} = 4.7 \times 10^{-6}/^\circ\text{C}$ ) [14, 15]. This thermal expansion effect seems to be responsible not only for the plastic deformation of the structure but also for the formation of microcracks. This effect might possibly be reduced by the building-in of a transition region.

According to the microscopic pattern the transition layer at the interface is most probably a homogeneous solid solution of ZnS-GaP, enriched in ZnS. This phenomenon is supported also by the fact that these compounds can easily form solid solutions in all compositions by similar transport reactions [5]. Since vapour etching of the substrates at the initial stage of the process results in GaCl, GaCl<sub>3</sub>, P<sub>2</sub> and P<sub>4</sub> in the gas phase, these components might build into the growing ZnS layer forming a mixed phase, similar to that described for the GaAs-Ge heteroepitaxial system [16].

### Acknowledgements

Acknowledgements are due to Dr G. Szigeti, Director of the Institute, to Dr G. Gergely, and Dr J. F. Póczy for valuable discussions. Thanks are due to J. Hagyló and P. Lórik for their kind assistance.

### References

1. J. T. CALLOW, P. J. DEASLEY, S. J. T. OWEN, and P. W. WEBB, *J. Materials Sci.* **2** (1967) 88.
2. W. KLEBER and J. MENDEL, *Z. Phys. Chem.* **231** (1966) 191.
3. P. L. JONES, C. N. W. LITTING, D. E. MASON, and V. A. WILLIAMS, *Brit. J. Appl. Phys.* **2** (1968) 283.
4. B. A. UNVALA, J. M. WOODCOCK, and D. B. HOLT, *ibid* **2** (1968) 11.
5. I. BERTÓTI, M. FARKAS-JAHNKE, M. HÁRSY, T. NÉMETH, and K. RICHTER, Proc. Int. Conf. on Luminescence (The Publishing House of the Hung. Acad. of Sci., Budapest, 1966) p. 1261.
6. I. BERTÓTI, M. FARKAS-JAHNKE, T. NÉMETH, and L. VARGA, to be published.
7. F. B. BAKRADZE and I. A. ROM-KRITSHEWSKAYA, *Kristallografiya* **8** (1963) 238.
8. H. W. STURNER and C. E. BLEIL, *Appl. Optics* **3** (1964) 1015.
9. A. I. BENNETT and R. L. LONGINI, *Phys. Rev.* **116** (1959) 53.
10. H. C. GATOS, P. L. MOODY, and M. C. LAVINE, *J. Appl. Phys.* **31** (1960) 212.
11. O. BRAFMAN, E. ALEXANDER, B. S. FRAENKEL, Z. H. KALMAN, and I. T. STEINBERG, *ibid* **35** (1964) 1855.
12. J. E. O'NEAL and F. W. LEONHARD, *J. Cryst. Growth* **2** (1968) 80.
13. J. WOODS, *Brit. J. Appl. Phys.* **11** (1960) 296.
14. R. R. REEBER and G. W. POWELL, *J. Appl. Phys.* **38** (1967) 1531.
15. M. E. STRAUMANIS, J. P. KRUMME, and M. RUBINSTEIN, *J. Electrochem. Soc.* **114** (1967) 1.
16. T. ARIZUMI and T. NISHINAGA, *Japan J. Appl. Phys.* **5** (1966) 21.